MedCrave
Step into the World of Research
Journal of Analytical & Pharmaceutical research

Research Article

Open Access
CrossMark

# Complexes formed between polyelectrolyte and acetylated cationic dendrimers

## Abstract

Gene therapies are receiving a revival, especially because of the potential for use in cancer and infectious disease vaccination. However, effectively condensing and maintaining deoxyribonucleic acid (DNA) carriers for gene therapy are used, such as dendrimers. The penetrable sphere model developed by Qamhieh et al., explain the interaction between linear polyelectrolyte (LPE) and an ion-penetrable sphere was employed to study the complexation of negatively charged DNA and acetylated dendrimer. Throughout the study, we emphasized the effect of acetylation on two types of complexations: single dendrimer-DNA chain complex and multiple dendrimers-DNA chain complex. The interaction between three different DNA lengths: L = 90 nm of 265; L = 184 nm of 541 bp; and L = 680 nm of 2000 bp individually with the poly (amido amine) (PAMAM) dendrimer of generation 5 was studied. For a single dendrimer-DNA complex, the number of condensed monomers around the dendrimer and the fraction of optimal length wrapping around the dendrimer was studied. It was found that by increasing acetylation, the number of condensed monomers and the fraction of optimal length decreased. For multiple dendrimers-DNA complex, the optimal length $l_{opt}$ wrapping around the dendrimer and the linker that forms between complexes were studied. As a result, with increasing acetylation, the $l_{opt}$ will shorten while the linker will increase significantly. The acetylation also affected the number of turns wrapping around the dendrimer and the net charge of the complex for single and multiple dendrimer-DNA complexes, and it was found that the longer the chain length, the more turns there are around the dendrimer. The net charge of all complexes was negative due to increased acetylation. In this study, it is revealed that the developed model is suitable for demonstrating the complexation between the dendrimer and the DNA.

**Keywords:** analytical model, linear polyelectrolyte, dendrimers, complexes, linker

Volume 12 Issue 2 - 2023

Raghad Natsha,[1] Khawla Qamhieh[2]
[1]Chemistry Department, College of science and technology, Al-quds University, Palestine
[2]Physics Department, College of science and technology, Al-quds University, Palestine

**Correspondence:** Raghad Natsha, Al-Quds University, Jerusalem, Palestine, Email raghad.natsheh12@gmail.com

**Received:** May 15, 2023 | **Published:** May 26, 2023

**Abbreviations:** LPE, linear polyelectrolyte; PAMAM, poly (amido amine); $l_{opt}$ , the optimal length; ds, double strand; ss, single strand

## Introduction

With the ability to insert synthetic genetic material such as DNA and RNA into target cells and cause the synthesis or inhibition of illness-related proteins), gene therapies are potent methods for treating or curing disease.[1] Because bare nucleic acids have poor intracellular transport and are vulnerable to nucleases, effective gene therapy relies on the efficient condensation, protection, and delivery of genetic material utilizing vectors and genetic carriers.[2]

There are two types of carriers: viral and non-viral vectors, which are both employed to deliver genetic material into body cells.[3] In situations where conventional immunomodulating therapies have failed to produce satisfactory results, biological carriers of genetic material, such as viral vectors, are successfully used in experimental gene therapies to treat immunodeficiencies or in the design of Chimeric Antigen Receptor T cell (CAR-T) receptors to eradicate cancer cells.[3,4] Nevertheless, the use of viral vectors in gene therapies is severely limited due to challenging large-scale production as well as a certain level of immunogenicity and carcinogenicity, so current scientific efforts are focused on the study of a broad range of molecules, such as dendrimers, which are able to carry genetic material into the cells.[3,5,6]

These dendrimers have a structure like a tree (hyperbranched). Between the branching sites, the internal layers from the dendrimer's core to the surface groups have a homogenous structure.[1] Poly(amido amine) (PAMAM) dendrimers currently considered as the most interesting ones among all dendrimers.[7] They are well-known for their hydrophilicity, flexibility, mechanical and chemical durability, and extensive surface functionality, and are ordered three-dimensional (3D) hyperbranched polymers with adjustable size and geometry.[8] PAMAM dendrimers can be produced using a variety of methods, such as divergent step-growth polymerization in a layer-by-layer fashion (referred to as "generations" or "G"), usually centered around an initiator 2-carbon ethylenediamine core unit (although ammonia and cystamine are also frequently employed core structures.[9,10] According to studies, PAMAM dendrimers with positive charges on their surfaces have higher transfection effectiveness because they are more permeable to cell membranes than their anionic and neutral versions. A very high level of cytotoxicity is also produced by such a cationic surface. Their surface amine group's ability to be functionalized has been said to have cytotoxicity-lowering effects.[7] In order to maximize PAMAM dendrimers' potential for applications involving the transport of nucleic acids while minimizing their cytotoxicity, it has been demonstrated that amine acetylation of cationic polymers reduces cytotoxicity in a range of different cell lines.[11]

G5 PAMAM dendrimer in particular is anticipated to play a significant role in regulating the characteristics of medicinal moieties and possess minimal toxicity. The inside and outside of the nanoparticulate architecture are hydrophilic. In fact, G5 PAMAM dendrimer partial acetylation can be utilized to neutralize the dendrimer surface, avoiding adverse reactions and nonspecific targeting from happening during device distribution while also enhancing the solubility of the dendrimer. The remaining primary amino groups that are not acetylated can be utilized to attach a variety of functional molecules, including medicinal medicines, imaging agents, and targeting molecules.[12]

Submit Manuscript | http://medcraveonline.com



©2023 Natsha et al. This is an open access article distributed under the terms of the Creative Commons Attribution License, which permits unrestricted use, distribution, and build upon your work non-commercially.

Copyright: ©2023 Natsha et al.



Several studies show how acetylation affects dendrimers. For instance, by using a coarse-grained model, Hwankyu and Ronald[13] investigated the effects of 0%, 50%, and 100% acetylation on the radii of gyration (Rg) of G3 and G5 dendrimers. They verified that the radii of gyration were calculated, and the findings show that once the simulations begin, the Rg values for dendrimers drastically decrease with time. Additionally, the higher acetylated G5 dendrimers display lower Rg values in comparison to unacetylated dendrimers.[13]

When the dendrimer's positive charge interacts electrostatically with negatively charged nucleic acid molecules, complexes are formed.[14-17] However, on the basis of electrostatic interactions, the complexes of dendrimers/polyelectrolytes have been studied extensively. For example, in investigations for determining and validating novel drug targets as well as examining gene activity, the transport of small interfering RNAs (siRNAs) into target cells utilizing PAMAM dendrimers has been shown.[18] Also, single nanoparticles (SNPs) containing PAMAM dendrimers were created. Cationic SNPs compress anionic DNA through electrostatic interactions. The findings show that the SNP/DNA polyplexes successfully transfected genes into a variety of cell lines, including U87, MCF-7, and 3 T3 cells.[19]

Vasumathi and Maiti used atomistic molecular dynamics based on free energy calculations and intrinsic structure determination to study the complexation between generation G3/G4 PAMAM and siRNA. Additionally, the complexation behavior was investigated utilizing various vector and siRNA combinations, namely one siRNA and two dendrimers (two G3 or two G4). Within nanoseconds, a stable siRNA dendrimer complex was created. The binding energy between siRNA and the dendrimer increased when dendrimer generation increased from three to four, potentially due to a high charge ratio. The scientists came to the conclusion that two G4 dendrimers had the highest binding affinity, whereas one PAMAM dendrimer of G4 and two PAMAM dendrimers of G3 formed the smallest complexes.[20,21] The complexation of dendrimers/polyelectrolytes also studied theoretically by Nguyen and Shklovskii[22,23,24,17] In this research, our goal is to study the compaction of acetylated dendrimers with a single DNA and other polyelectrolytes and investigate the conformation of the DNA-Dendrimer complex by applying the penetrable sphere analytical model developed by Qamhieh et al.[25] However, depending on what Yu and Larson[26] studied about the effect of acetylation on dendrimer radius and found that the dendrimer radius decreases and compresses when the acetylation percentage is increased. As a result, the dendrimer's positive charge is reduced. We used this data to build our findings.

## Analytical model

A penetrable sphere model developed by Qamhieh et al.[15] describing the complexation of penetrable spheres and linear poly electrolyte (LPE) chain was adopted to study the conformation of the complexes resulting of the compaction of the DNA with the acetylated G5 dendrimer. The model is developed by replacing the hard spheres in Schiessel's model,[24] by soft (penetrable) spheres to represent the flexible dendrimers. In penetrable sphere, the charge should be distributed evenly through the whole volume, and the linear chain charges should have the possibility to be localized near the opposite charges inside the sphere. The polyelectrolyte chain is considered as a rod of radius r = 1 nm, length $L$, persistence length $lp$, and the charge density is $-e/b$, where b is the axial spacing between charges, and the dendrimer as an ion penetrable sphere of radius $R$ and charge Ze. The sphere and the LPE chain are placed in a system characterized by Bjirrum length $l_B = e^2 / 4\pi\varepsilon k_B$, and a Debye screening length (DSL): $\kappa^{-1} = \left(8\pi C_s l_B\right)^{-1/2}$, where ε is the dielectric constant of the solvent, $C_s$ is the salt concentration, and $k_B T$ is the thermal energy. The complexation in our study is carried out in 10 mM 1:1 salt aqueous solution, so $\kappa^{(-1)} = 3$ nm, and $l_B = 0.7$ nm using the dielectric constant of water at room temperature ε = 78.4. Here, the penetrable sphere model is applied to obtain mechanistic understanding of how the acetylation affects the fraction of the DNA wrapping round the dendrimer, which in turn will influence on the formation and structure of DNA-dendrimer aggregates. A semiflexible ($lp$ = 50) single strand DNA (ssDNA) (b=0.34) and double strand DNA (dsDNA) (b=0.17) with three lengths, 90 nm 265 bp, 184 nm 541 bp, and 680 nm (2000 bp DNA) were used in this study. The properties of acetylated G5 dendrimer used are shown in Table 1, where the values of the radii $R_s$ are adopted from a Monte Carlo (MC) simulation done by Yu, S.,[26] to investigate the acetylated G5 dendrimer in 10 mM salt aqueous solution. They concluded that radius of gyration ($R_g$) decreases almost linearly for a low degree of acetylation < 50 %, while for higher degrees of acetylation, a near-plateau in dendrimer size is ultimately attained. A fully neutralized G5 dendrimer has a 22% smaller $R_g$ than a nonacetylated dendrimer. As a consequence, for the acetylation, the positive charge of the dendrimer is reduced from 128 $e$ at zero acetylation to 12.8 $e$ at 90% acetylation as shown in Table 1.[27]

**Table 1** Properties of the G5 dendrimer G investigated in Raghad AbdalMuiz Natsha's thesis[27]

| *Acetylation %* | $R_s\,(nm)$ | $Z(e)$ | $ó\left(e/nm^2\right)$ | $l_{iso}$ ssDNA | $l_{iso}$ dsDNA |
|---|---|---|---|---|---|
| 0 | 2.67 | 128.0 | 1.43 | 43.52 | 21.76 |
| 10 | 2.58 | 115.2 | 1.38 | 39.17 | 19.58 |
| 20 | 2.50 | 102.4 | 1.30 | 34.82 | 17.41 |
| 30 | 2.42 | 89.6 | 1.22 | 30.46 | 15.23 |
| 40 | 2.35 | 76.8 | 1.11 | 26.11 | 13.06 |
| 50 | 2.24 | 64.0 | 1.02 | 21.76 | 10.88 |
| 60 | 2.18 | 51.2 | 0.86 | 17.41 | 8.70 |
| 70 | 2.14 | 38.4 | 0.67 | 13.06 | 6.53 |
| 80 | 2.11 | 25.6 | 0.46 | 8.70 | 4.35 |
| 90 | 2.07 | 12.8 | 0.24 | 4.35 | 2.18 |

$R_s$ is the radius of the dendrimer, and [a] $Z$ is the number of charged group, [a] $\sigma$ is the surface charge density of the dendrimer, and [a] $l_{iso}$ is the isoelectric length of the ssDNA and dsDNA, i.e. the length of the DNA required to neutralize the charge of the different dendrimer.

**Citation:** Natsha R, Qamhieh K. Complexes formed between polyelectrolyte and acetylated cationic dendrimers. *J Anal Pharm Res.* 2023;12(2):80–87. DOI: 10.15406/japlr.2023.12.00427

Copyright: ©2023 Natsha et al.



### Calculation of the free energy for the dendrimer/DNA complex

The total free energy of a system made up of one sphere and one linear chain according to Schiessel's model,[24] is represented as follows:

$$F(l) = F_{compl}(l) + F_{chain}(L-l) + F_{compl-chain}(l) + F_{elastic}(l) \quad (1)$$

Where $(L-l)$ is the length of the remaining chain, and $l$ is the length of the segment of the DNA molecule that is wrapped around the sphere. When the sphere is modeled as a soft sphere (ion penetrable sphere), the first term is the electrostatic charging free energy of spherical complex of charge $Z(l)e$ :

$$F_{compl}(l) = \frac{3}{8\pi}\frac{Z^2(l)K_BT}{(kR)^2}\frac{exp(kR)l_B}{R}\left[\cosh(kR) - \frac{\sinh(kR)}{kR}\right]\frac{e^{-kR}}{R} \quad (2)$$

To calculate the complex's overall charge, we used:

$$Z(L) = Z - L/b$$

In this case, the complex stands for the wrapped chain that corresponds to the sphere. The remaining chain's $(L-l)$ second term of total entropic electrostatic free energy may be calculated as follows:

$$F_{chain}(L-l) \cong \frac{K_BT}{b}\Omega(a)\left(1-\xi^{-1}\right)(L-l) \quad (3)$$

$$\Omega(a) = \ln\left(4\xi k^{-1}\right)/a \quad (4)$$

where $\Omega$ (a) represents the entropic cost to "confine" counterions near the chain. The Manning parameter is defined as $\xi = l_B/b$ . The third term, which is the resultant free energy between the complexes (shown as soft spheres) and the unwrapped LPE chain fragment, may be expressed as follows:

$$U_{compl-chain}(l)/k_BT \cong \frac{3Z(l)l_B}{4\pi(kR)^2}\left[\cosh(kR) - \frac{\sinh(kR)}{kR}\right] \times \left[\ln(r) - \sum_{n=0}^{\infty}\frac{(-1)^n}{(n+1)!.(n+1)}(kr)^{n+1}\right]\Bigg|_{R}^{L-Nl} \quad (5)$$

Similar to the term used in Scheissel's model,[24] the last term in Eq. (2.1), $F_{elastic}(l)$, represents the elastic free energy needed to bend $l$ of the chain of radius of curvature around a sphere of radius R:

$$F_{elastic}(l) \cong \frac{K_BTl_p}{2R^2}l \quad (6)$$

### Free energy calculation for a complexation between a LPE chain and multiple dendrimers

For a system with one LPE chain and N spheres, the total free energy can be obtained by:

$$F(N,l) = NF(l) + F_{int}(N,l) \quad (7)$$

where $F_{\text{int}}$ is the electrostatic interaction between the spheres, that decorate the LPE chain. It can be determined by combining the electrostatic repulsion between all complexes within a single chain. Based on the study for Qamhieh et al.,[17] the free energy interaction between two penetrable spheres is given by:

$$F_{int}(N,l) = \frac{9Z^2(l)K_BTl_B}{8\pi(kR)^4}\left[\cosh(kR - \frac{\sinh(kR)}{kR}\right]^2 \times \sum_{i=1}^{N-1}\left[\left[\frac{N-i}{i}\right]\frac{e^{-kD(N,l)}}{D(N,l)}\right] \quad (8)$$

Where the center-to-center distance between two nearby complexes is given by $(N,l) = (L - Nl + 2NR)/N$ . The system's overall free energy may be expressed as follows:

$$\frac{F(N,l)}{K_BT} = \left\{\frac{3}{4\pi}\frac{NZ(l)l_BA}{(kR)^2}\left[\frac{Z(l)e^{-kR}}{2R} + \frac{1}{b}\int_R^{L-Nl}\frac{e^{-kr}}{r}dr + \frac{3Z(l)A}{2(kR)^2}\sum_{i=1}^{N-1}X_i\left\{\frac{N-i}{i}\right\}\frac{e^{-kD(N,l)}}{D(N,l)}\right] + \frac{1}{b}\Omega(a)\left(1-\xi^{-1}\right)(L-Nl) + \frac{Nl_p}{2R^2}l\right\} \quad (9)$$

### Software analysis

Various computational software applications are utilized to carry out these calculations. Some of the theoretical results were graphed and examined using the Qtgrace program version 5.6.0.[28] The mathematical tool Maple version 2021.[29] was used in the current work to carry out the method of optimization of the total free energy for a system of LPE chains interacting with penetrable spheres. To extract values from several graphs from earlier investigations, the Get Data Digitizer tool, version 2.26.0.20,[30] was also employed.[27]

## Results and Discussion

In order to calculate the optimal wrapping length ($l_{opt}$) of DNA around a dendrimer, Eq. 9 can be solved by taking its first derivative with respect to the wrapping length $l$ and equating it to zero. In our study all the systems are at room temperature.

### Effect of acetylation on single PAMAM dendrimer–DNA complex conformation

The complexation of ssDNA and dsDNA chains of three lengths of (L = 90, 184, and 680 nm) with one acetylated G5 dendrimer (PAMAM EDA-core) in a 10 mM 1:1 salt solution corresponding to a DSL of 3 nm with $l_B$ of 0.71 nm has been investigated by the penetrable sphere model. The semiflexible ssDNA and dsDNA chains have $lp = 50$ nm with b = 0.34 nm, and b = 0.17 nm respectively. The number of monomers condensed on the dendrimer can be found by dividing the wrapping length $l_{opt}$ by the space between monomers b, as shown in Figure 1a, which demonstrates that by increasing acetylation, a decrease in the number of condensed DNA chain monomers around the dendrimer was found when using all the chain lengths of 90, 184 and 680 nm for both ssDNA and dsDNA chains. While the fraction of optimal length wrapping around the dendrimer can be found by dividing the wrapping length $l_{opt}$ by the DNA chain length L and is shown in Figure 1b, which reveals that this fraction becomes less wrapped around the dendrimer by decreasing $R_s$ resulted by increasing acetylation as predicted by Qamhieh and colleagues,[17] it is shown that the optimal DNA wrapping length does indeed decrease with $R_s$ .

The effect of acetylation on the number of DNA chain turns around single dendrimer and on the net charge of the single dendrimer-DNA complex was studied. The number of DNA chain turns around the dendrimer can be calculated by using the optimal wrapping length $l_{opt}$ divided by the circumference $2\pi R_s, (l_{opt}/2\pi R_s)$, as shown in Figure 2a, which illustrates that complexes using a chain length of 90 nm to wrap around one dendrimer have a slight increase in turns in the case of using ssDNA and dsDNA chains up to 40% acetylation, but after this percent, the dsDNA chain has a greater number of turns than the ssDNA chain. In addition, we note a slight decrease after 60% acetylation was found in the case of using ssDNA. For a chain length of 184 nm, the number of turns for the dsDNA was

**Citation:** Natsha R, Qamhieh K. Complexes formed between polyelectrolyte and acetylated cationic dendrimers. *J Anal Pharm Res.* 2023;12(2):80–87.
DOI: 10.15406/japlr.2023.12.00427

Copyright: ©2023 Natsha et al.



higher than for the ssDNA. Also, the number of turns increases at the beginning of acetylation until reaching 40% acetylation in the case of using both ssDNA and dsDNA chains. Following this percentage, the number of turns decreases by increasing acetylation when using ssDNA, whereas it remains constant when using dsDNA. In the case of using the chain of length 680nm, the number of turns decreased by increasing acetylation, and the dsDNA chain has a greater number of turns than the ssDNA chain around the dendrimer. We come to the conclusion that using a dsDNA chain gives a higher number of turns around the dendrimer due to the presence of more negative charges, which improves overcharging with the dendrimer's positive charge. Additionally, the longer the chain length, the more turns there are around the dendrimer, as revealed by the results when using a chain length of 680 nm, since the longer chain has more negative charges. The net charge of the complex can be found by combining the charge of the dendrimer $Z_d$ and the charge of the DNA chain wrapping around the dendrimer $Z_{l_{opt}}$, $(Z^* = Z_d + Z_{l_{opt}})$, as shown in Figure 2b, which illustrates that in the case of using chain lengths of 90, 184, and 680 nm with one dendrimer, we notice that the net charge of all complexes was negative by increasing acetylation. This means that the charge on the dendrimer is inverted, and the complexes containing a dsDNA chain are more negative than those using ssDNA. For complexes using a chain length of 90 nm, it was revealed that the net charge increases in negativity by increasing acetylation for both ssDNA and dsDNA chains. Whereas for complexes using a chain length of 184 nm, there is an increase in negative charge at the beginning of acetylation until it reaches 40% and 30% when using both ssDNA and dsDNA, respectively. After these percentages, a decrease in negative charge was found by increasing acetylation. Furthermore, in the case of using a chain length of 680 nm, a decrease in negative charge was found by increasing acetylation from the start to the end of acetylation when using both ssDNA and dsDNA chains.

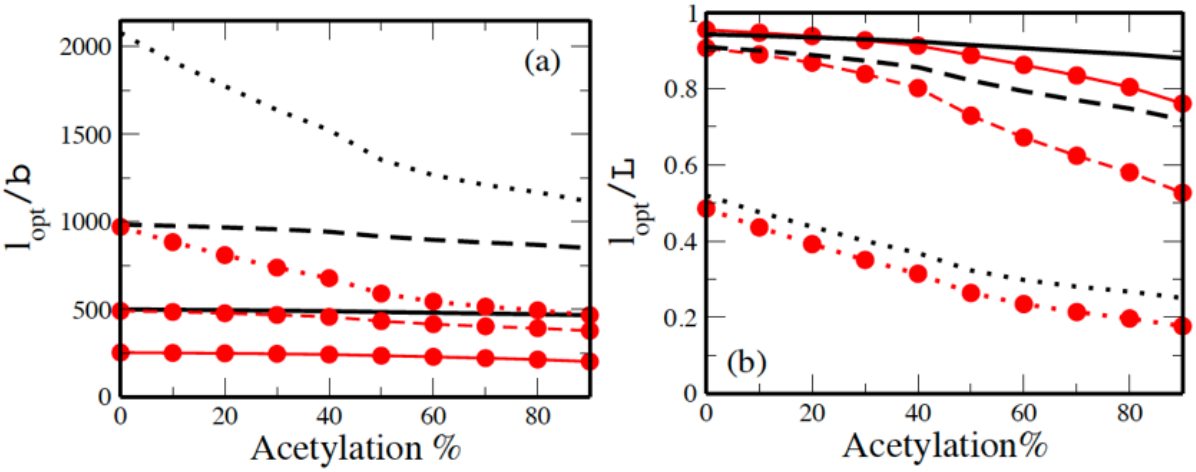


**Figure 1** a) The number of condensed monomers as a function of acetylation %, and b) Fraction of optimal length lopt/L as a function of acetylation %. The lengths of semiflexible ssDNA, shown as lines with symbols, and semiflexible dsDNA, shown as lines without symbols, L = 90 nm (Solid lines), L =184 nm (dashed lines), and L = 680 nm (dotted lines).

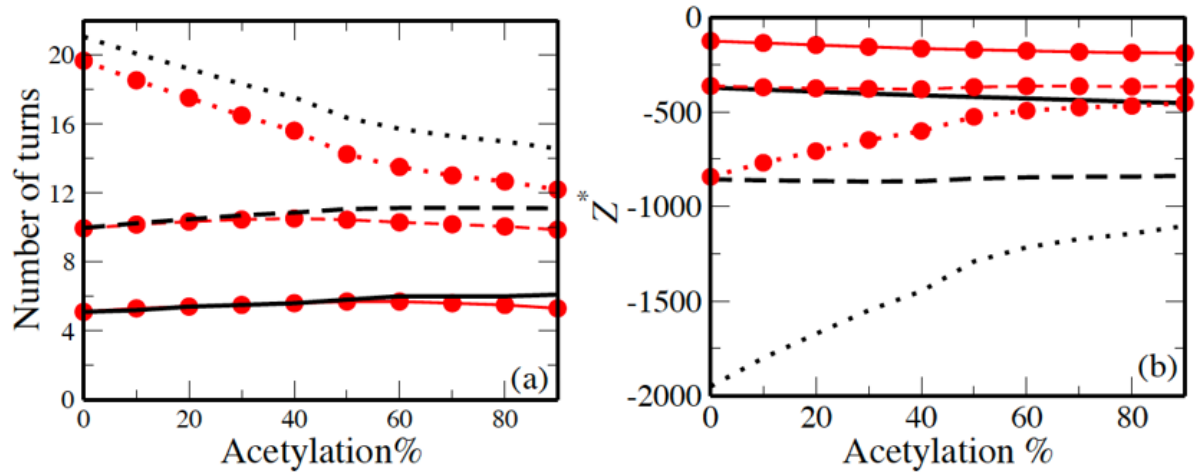


**Figure 2** a) Number of turns on the dendrimer around DNA chain as a function of acetylation %, and b) The net charge of the complex Z* (Zcomplex) as a function of acetylation %, when N=1. The lengths of semiflexible ssDNA, shown as lines with symbols, and semiflexible dsDNA, shown as lines without symbols, L = 90 nm (Solid lines), L =184 nm (dashed lines), and L = 680 nm (dotted lines).

## Effect of acetylation on multiple PAMAM dendrimer – DNA complex conformation

The complexation of ssDNA and dsDNA chains of two different lengths of (L =184, and 680 nm) with multiple acetylated G5 dendrimers (PAMAM EDA-core) with N= 1-6, in a 10 mM 1:1 salt solution corresponding to a DSL of 3 nm with a $l_B$ of 0.71 nm has been investigated by the penetrable sphere model. The semiflexible ssDNA and dsDNA chains have $lp = 50$ nm with b = 0.34 nm, and

**Citation:** Natsha R, Qamhieh K. Complexes formed between polyelectrolyte and acetylated cationic dendrimers. *J Anal Pharm Res.* 2023;12(2):80–87. DOI: 10.15406/japlr.2023.12.00427

Copyright: ©2023 Natsha et al.



b = 0.17 nm respectively. The effect of acetylation on the $l_{opt}$ around dendrimer N and on the linker formed between complexes has been studied. According to the information in Table 1, as the acetylation % increases, the $R_s$ will decrease resulting in a smaller, more compact dendrimer. From Figures 3 and 4, we can see that with increasing acetylation, the $l_{opt}$ wrapping around the dendrimer will shorten while the linker that forms from the remaining unwrapped chain between complexes will increase significantly. Additionally, we observe that as the number of these dendrimers increases, the $l_{opt}$ wrapping around them and the length of the linker between complexes both become shorter with increasing acetylation. as revealed by Qamhieh et al.,[14] In addition, when the number of dendrimers was increased, the ssDNA chain had a greater decrease in the $l_{opt}$ than the dsDNA chain at higher acetylation percentages. On the other hand, shorter linker length was found in the case of using dsDNA chain. Furthermore, for complexes of length 184 nm with N = 5 and 6, the $l_{opt}$ of the ssDNA chain begins to wrap at 20% and 30% acetylation, respectively. This is because at low acetylation percentages, dendrimers have larger radii and the utilized chain length is insufficient to wrap around 5 and 6 dendrimers until their radii are reduced. In fact, as demonstrated by the research of Qamhieh and colleagues, utilizing more dendrimers necessitates additional negative charges that come from the DNA chain for neutralizing and wrapping.[14]

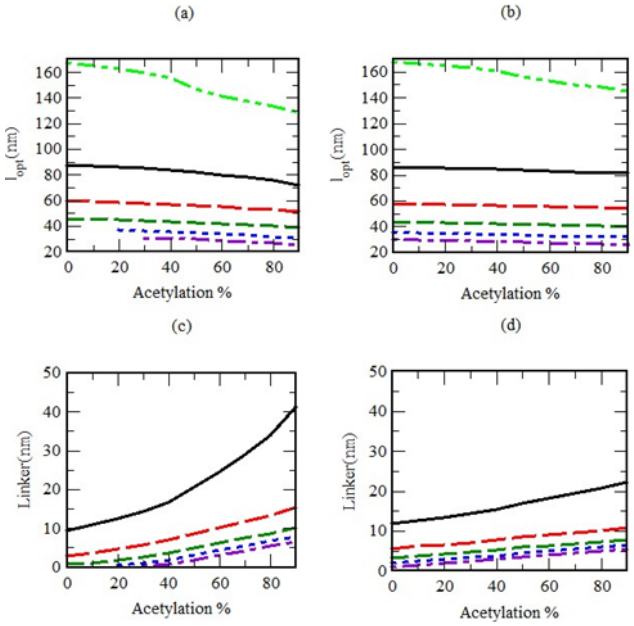


**Figure 3** (a) and (b) $l_{opt}$, and (c) and (d) Linker formed when NG5 acetylated dendrimers compacted with 184 nm semiflexible ssDNA (b=0.34) (a) and (c), and semiflexible dsDNA (b=0.17) (b) and (d), as a function of acetylation %. %. N = 1, N = 2, N = 3, N = 4, N = 5, and N = 6.

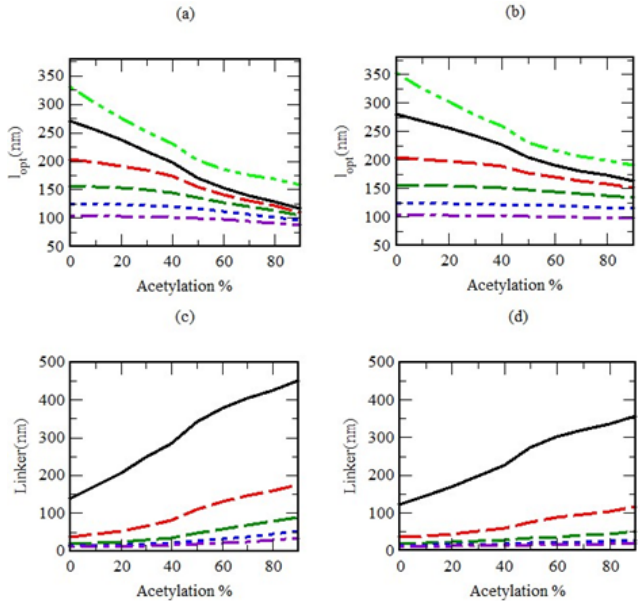


**Figure 4** (a) and (b) $l_{opt}$, and (c) and (d) Linker formed results of condensing 680 nm semiflexible ssDNA (b=0.34) (a) and (c), and semiflexible dsDNA (b=0.17) (b) and (d) as a function of acetylation %. N = 1, N = 2, N = 3, N = 4, N = 5, and N = 6.

The effect of acetylation on the net charge of the multiple dendrimers - DNA complex and on the number of DNA chain turns around multiple dendrimers was studied. Figure 5 illustrates the complex compacted with a chain length of 184 nm in the case of using both ssDNA and dsDNA chains, and it was discovered on Figures 5a and 5b that all complexes had a negative net charge. With the exception of the complex containing a single dendrimer (N=1), an increase in negativity was seen at the beginning of acetylation till reaching 40% and 30%, when employing ssDNA and dsDNA chains respectively. Following these percentages, there is a slight decrease in the negative charge. From Figure 5c, the number of turns in the case of using ssDNA chain increase by increasing acetylation until reaching 40% and 60% acetylation when using single and double dendrimers respectively. After that a small decrease was found. But by increasing the number of dendrimers to 3, the number of turns increased slightly at the beginning of acetylation, up to 20%, before becoming about constant. Then, using a greater number of dendrimers resulted in a constant number of turns. From Figure 5d when a dsDNA chain was used, the number of turns wrapping around a single dendrimer was slightly increased by increasing acetylation until reaching 40%, at which point it remained constant. While when the chain wrapping around 2 and 3 dendrimers a small increase in turns was found by increasing acetylation till the end of acetylation. Furthermore, when utilizing dendrimers more than 3, the number of turns become constant at all acetylation %. We can conclude that by increasing acetylation, the number of turns of the ssDNA and the dsDNA chains become around constant when wrapping around multiple dendrimers.

Figure 6 illustrates the complex compacted with a chain length of 680 nm in the case of using both ssDNA and dsDNA chains. The effect of acetylation on the complex net charge is revealed in Figures 6a and 6b. From Figure 6a, all complexes' net charge is negative, and we can notice that for complexes that include dendrimers with N = 1 - 3 in the case of using the ssDNA chain, the net charge of the complex decreases slightly in negativity by increasing acetylation. Also, complexes included dendrimers with N = 4 and 5, the charge of these complexes decreases in negativity when the acetylation % rises to 40% and 50%, respectively. While the complex included 6 dendrimers, the charge of the complex was negative and increased in negativity. From Figure 6b all complexes have a negative charge, and we can notice that for complexes that include dendrimers with N = 1 - 3 in the case of using the dsDNA chain, the net charge of the complex decreases

**Citation:** Natsha R, Qamhieh K. Complexes formed between polyelectrolyte and acetylated cationic dendrimers. *J Anal Pharm Res.* 2023;12(2):80–87. DOI: 10.15406/japlr.2023.12.00427

Copyright: ©2023 Natsha et al.



slightly in negativity by increasing acetylation. While for the complex that includes 4 dendrimers, the charge decreases in negativity after 50% acetylation, in the case of using 5 and 6 dendrimers, the charge increases in negativity by increasing acetylation.

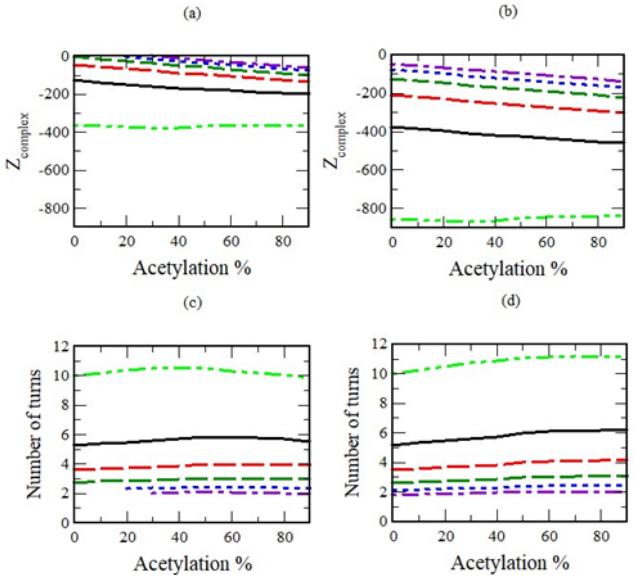


**Figure 5** (a) Net charge, and (b) number of turns on a complex formed when NG5 dendrimers compacted with 184 nm semiflexible ssDNA (b=0.34) (a) and (c), and semiflexible dsDNA (b=0.17) (b) and (d), as a function of acetylation %. N = 1, N = 2, N = 3, N = 4, N = 5, and N = 6.

The effect of acetylation on the number of turns is illustrated in Figures 6c and 6d. From Figure 6c, in the case of using the ssDNA chain, the number of turns is decreased by increasing acetylation when utilizing dendrimers with N =1, 2 and 3. When using dendrimers with N = 4, 5, and 6, the decrease in turns was found after 40%, 50%, and 70% acetylation, respectively. But below these percents, increasing the number of turns was found by increasing acetylation. From Figure 6d, in the case of using a dsDNA chain, the number of turns is decreased by increasing acetylation when using dendrimers with N = 1,2 and 3. When using dendrimers with N = 4, the number of turns decreases by increasing acetylation above 40%, and for the dsDNA chain wrapping around 5 and 6 dendrimers the number of turns was found to be around constant after 60% and 70% acetylation respectively. On the other hand, below these percents in the case of using N = 4,5 and 6, the number of turns was increased by increasing acetylation.

To conclude the results in Figures 5 and 6, by increasing acetylation, the net charge of complexes using the dsDNA chain is more negative than that of those using the ssDNA chain, this is due to more negative charges on the dsDNA chain. Also, the longer chain length of 680 nm, gives us better overcharging with dendrimers by increasing acetylation than the shorter length of 184 nm. Furthermore, for the complexes that include a low number of dendrimers, we can notice that they have more negative charges than the charges of complexes that hold a higher number of dendrimers. We therefore speculate that this is due to the positive charge that is held by the dendrimer, and by increasing the number of dendrimers, this led to a decrease in the negative charge of the complex. On the other hand, the more complex negative charge reveals more overcharging between the chain and dendrimer, which means a higher number of turns. For instance, we can see from Figures 6b and 6d that the complex including N=1 has the highest complex net charge. Also, it has a greater number of turns wrapping around the dendrimer. These results reveal the importance of the net charge of the complexes, which is considered an important parameter for gene delivery applications and can be estimated based on the DNA wrapping length.

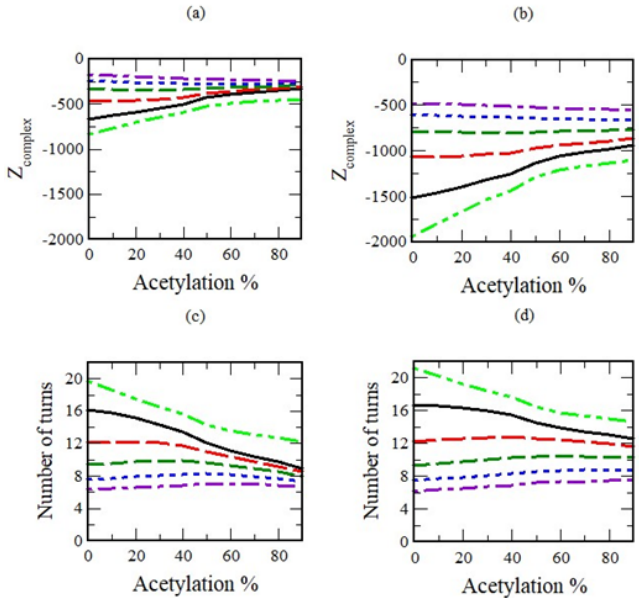


**Figure 6** (a) Net charge, and (b) number of turns on one complex formed when NG5 dendrimers with 680 nm semiflexible ssDNA (b=0.34) (a) and (c), and semiflexible dsDNA (b=0.17) (b) and (d), as a function of acetylation %. N = 1, N = 2, N = 3, N = 4, N = 5, and N = 6.

The number of turns wrapping around a dendrimer for complexes using a chain length of 680 nm in the case of using dsDNA, and a number of dendrimers ranging from 2 to 6 is illustrated in 3D images at 0%, 40%, and 90% acetylation in Figures 7, 8 and 9, respectively.

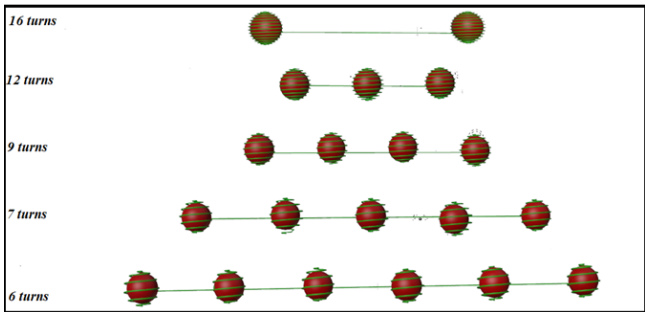


**Figure 7** Number of turns of dsDNA chain on the dendrimer at zero % acetylation, when N=2, 3, 4, 5, and 6 and L=680 nm.

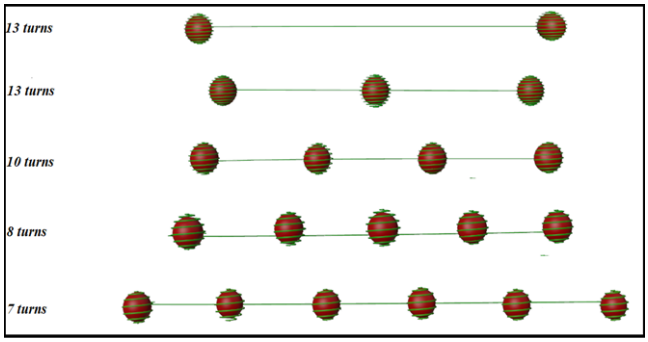


**Figure 8** Number of turns of dsDNA chain on the dendrimer at 40 % acetylation, when N=2, 3, 4, 5, and 6 and L=680 nm.

**Citation:** Natsha R, Qamhieh K. Complexes formed between polyelectrolyte and acetylated cationic dendrimers. *J Anal Pharm Res.* 2023;12(2):80–87. DOI: 10.15406/japlr.2023.12.00427

Copyright: ©2023 Natsha et al.



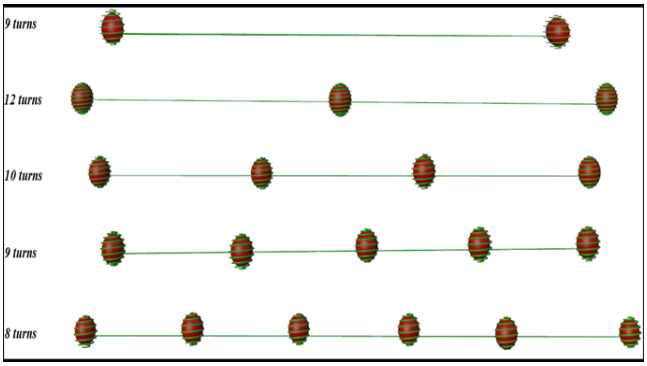


**Figure 9** Number of turns of dsDNA chain on the dendrimer at 90 % acetylation, when N=2, 3, 4, 5, and 6 and L=680 nm.

## Conclusion

The theoretical study that we have provided here is the first theoretical investigation that has accounted for the interaction of an oppositely acetylated penetrable charged sphere (dendrimer) with a semiflexible polyelectrolyte as a model of DNA. The acetylation markedly influenced the complex's final structure, including the dendrimer and the DNA chain, by decreasing the size and the charge of the G5 dendrimer. We studied the complexation of a single dendrimer with the DNA chain lengths of 90, 184, and 680 nm. The number of condensed monomers around the dendrimer and the fraction of the optimal wrapping length to the chain length both decrease as the acetylation percentage increases. The complexation of multiple dendrimers with the DNA chain lengths of 184 and 680 nm also investigated; our findings show that as the acetylation percentage increases, the optimal length decreases and the linker increases. Our results are in excellent agreement with those from earlier studies by Qamhieh. The effect of acetylation on the number of turns wrapping around the dendrimer and on the complex's net charge applied on two systems: the single dendrimer-DNA chain complex and the multiple dendrimers-DNA chain complex. As a result, by increasing acetylation, the longer the chain length of 680 nm, the more turns were found. Additionally, the net charge of all complexes was negative by increasing acetylation, and the complexes containing a dsDNA chain are more negative than those using ssDNA. Furthermore, we can see that the charges of the complexes with a small number of dendrimers are more negative than those of complexes with a larger number of dendrimers. As we speculated, this is because each dendrimer carries a positive charge, and adding more dendrimers resulted in a reduction in the complex's negative charge. More overcharging between the chain and dendrimer means a higher number of turns. The current analytical work, however, appears to be an intriguing subject for future gene therapy research and has important practical applications.

## Acknowledgments

None.

## Conflicts of interest

Authors declare that there is no conflict of interest.

## References

1. Caminade AM, Turrin CO, Majoral JP. Dendrimers and DNA: combinations of two special topologies for nanomaterials and biology. *Chemistry.* 2008;14(25):7422–7432.
2. Saviano F, Lovato T, Russo A, et al. Ornithine–derived oligomers and dendrimers for in vitro delivery of DNA and ex vivo transfection of skin cells via saRNA. *Journal of Materials Chemistry B*. 2020;8(22):4940–04949.
3. Tarach P, Janaszewska A. Recent advances in preclinical research using PAMAM dendrimers for cancer gene therapy. *International Journal of Molecular Sciences*. 2021;22(6):2912.
4. Milone MC, O'Doherty U. Clinical use of lentiviral vectors. *Leukemia.* 2018;32:1529–1541.
5. Sung YK, Kim SW. Recent advances in the development of gene delivery systems. *Biomaterials Research*. 2019;23(8).
6. Luo K, He B, Wu Y, et al. Functional and biodegradable dendritic macromolecules with controlled architectures as nontoxic and efficient nanoscale gene vectors. *Biotechnol Adv*. 2014;32(4):818–830.
7. Yan X, Yang Y, Sun Y. Dendrimer applications for cancer therapies. *Journal of Physics*. 2021;1948(1):012205.
8. Liu, X, Qiu, Y, Jiang, D, et al. Covalently grafting first–generation PAMAM dendrimers onto MXenes with self–adsorbed AuNPs for use as a functional nanoplatform for highly sensitive electrochemical biosensing of cTnT. *Microsystems & Nanoengineering.* 2022;8(1):35.
9. Araújo RVD, Santos SDS, Igne Ferreira E, et al. New advances in general biomedical applications of PAMAM dendrimers. *Molecules.* 2018;23(11):2849.
10. Kheraldine H, Rachid O, Habib AM, et al. Emerging innate biological properties of nano–drug delivery systems: A focus on PAMAM dendrimers and their clinical potential. *Advanced Drug Delivery Reviews.* 2021;178:113908.
11. Waite CL, Sparks SM, Uhrich KE, et al. Acetylation of PAMAM dendrimers for cellular delivery of siRNA. *BMC biotechnology*. 2009;9(38):1–10.
12. Yue Y, Eun JS, Lee MK, et al. Synthesis and characterization of G5 PAMAM dendrimer containing daunorubicin for targeting cancer cells. *Arch pharm res*. 2012;35(2):343–349.
13. Lee H, Larson RG. Molecular dynamics simulations of PAMAM dendrimer-induced pore formation in DPPC bilayers with a coarse-grained model. *J Phys Chem B.* 2006;110(37):18204-18211.
14. Qamhieh K, Nylander, Ainalem ML. Analytical model study of dendrimer/DNA complexes. *Biomacromolecules*. 2009;10(7):1720–1726.
15. Qamhieh K, Nylander T, Black CF, ET AL. Complexes formed between DNA and poly (amido amine) dendrimers of different generations–modelling DNA wrapping and penetration. *Physical Chemistry Chemical Physics*. 2014;16(26):13112–13122.
16. Mohammadinejad R, Dehshahri A, Madamsetty VS, et al. *In vivo* gene delivery mediated by non–viral vectors for cancer therapy. *Journal of Controlled Release.* 2020;325:249–275.
17. Qamhieh K. Analytical study of Linker Formation in Complexation of Two Dendrimers and one Polyelectrolyte. *Al–Quds Journal for Natural Sciences*. 2022;1(2).
18. Liu XX, Rocchi P, Peng L. Dendrimers as non–viral vectors for siRNA delivery. *New J Chem*. 2012;36:256–263.
19. Wang H, Chen KJ, Wang S, et al. A small library of DNA–encapsulated supramolecular nanoparticles for targeted gene delivery. *Chemical communications*. 2010;46(11):1851–1853.
20. Vasumathi V, Maiti PK. Complexation of siRNA with dendrimer: a molecular modeling approach. *Macromolecules*. 2010;43(19):8264–8274.

Copyright: ©2023 Natsha et al.




21. Kesharwani, P, Banerjee, S, Gupta, U, et al. PAMAM dendrimers as promising nanocarriers for RNAi therapeutics. *Materials Today.* 2015;18(10):565–572.
22. Nguyen TT, Shklovskii BI. Complexation of a polyelectrolyte with oppositely charged spherical macro– ions: giant inversion of charge. *The Journal of Chemical Physics.* 2001;114:5905–5916.
23. Rosen HR, Urbarz C, Holzer B, et al. Sacral nerve stimulation as a treatment for fecal incontinence. *Gastroenterology*. 2001;121(3):536–541.
24. Schiessel H, Bruinsma RF, Gelbart WM. Electrostatic complexation of spheres and chains under elastic stress. *The Journal of Chemical Physics*. 2001;115:7245–7252.
25. Qamhieh K, Khaleel AA. Analytical model study of complexation of dendrimer as an ion penetrable sphere with DNA. *Colloids and Surfaces A: Physicochemical and Engineering Aspects*. 2014;442:191–198.
26. Yu S, Larson RG. Monte–Carlo simulations of PAMAM dendrimer–DNA interactions. *Soft Matter*. 2014;10(29):5325–5336.
27. Natsha RAD. *Complexes formed between polyelectrolyte and acetylated cationic dendrimers* (Doctoral dissertation, Al-Quds University). 2022.
28. Winter. QtGrace - Browse files at SourceForge.net. QtGrace - browse files at SourceForge.net. 2017.
29. Bernardin CJ, Lewis T, Bell D, et al. Associations between social camouflaging and internalizing symptoms in autistic and non-autistic adolescents. *Autism.* 2021;25(6):1580-1591.
30. Fedorov VD, Themeli M, Sadelain M, PD-1- and CTLA-4-based inhibitory chimeric antigen receptors (iCARs) divert off-target immunotherapy responses. *Sci Transl Med.* 2013;5(215):215ra172.


**Citation:** Natsha R, Qamhieh K. Complexes formed between polyelectrolyte and acetylated cationic dendrimers. *J Anal Pharm Res.* 2023;12(2):80–87.
DOI: 10.15406/japlr.2023.12.00427